ELSEVIER

Contents lists available at ScienceDirect

Deep-Sea Research Part I

journal homepage: www.elsevier.com/locate/dsri





Using a Lagrangian particle tracking model to evaluate impacts of El Niño-related advection on euphausiids in the southern California Current System

Laura E. Lilly ^{a,*}, Bruce D. Cornuelle ^b, Mark D. Ohman ^a

- ^a Integrative Oceanography Division (IOD) and California Current Ecosystem Long-Term Ecological Research Site (CCE-LTER), Scripps Institution of Oceanography, University of California, San Diego, La Jolla, CA, USA, 92093
- b Climate, Atmospheric Sciences, and Physical Oceanography, Scripps Institution of Oceanography, University of California, San Diego, La Jolla, CA, USA, 92093

ARTICLE INFO

Keywords:
California current system
Euphausiids
Advection
Particle tracking model
El Niño
2014-15 warm anomaly

ABSTRACT

We propose a framework to examine the extent to which advection alone can explain spring biomass fluctuations of six euphausiid species in the southern California Current System (CCS) between 2008 and 2017. We modeled population changes as fluxes from defined source boxes using currents from the California State Estimate (CASE), a regional optimization of the MIT general circulation model. This period encompasses a Central Pacific El Niño (2009-10), Warm Anomaly (2014-15) and Eastern Pacific El Niño (2015-16). Total spring populations of all six species show strongest positive correlations with time-lagged flows from the preceding November-December. Three cool-water species (Euphausia pacifica, Nematoscelis difficilis, Thysanoessa spinifera) show opposite patterns for their calyptopis (larval) and adult phases, with strongest positive correlations of calyptopes with February-March flow suggesting periods of in situ reproduction. In contrast, three subtropical species (Nyctiphanes simplex, Euphausia eximia, Euphausia gibboides) show consistent correlation patterns with flow across the adult and calyptopis phases, suggesting advection of entire populations into the region during periods of enhanced favorable flows. We tested whether interannual variations in spring population size were influenced by different winter-origin waters during El Niño compared to non-Niño years. We found that cool-water species associate less strongly and subtropical species associate more strongly with southern-origin waters during anomalous years. Advection alone accounts for varying proportions of species fluctuations, with strongest influences for N. difficilis and T. spinifera. Explicit measurements of growth and mortality rates are needed to further resolve the additional factors influencing euphausiid populations during anomalous events, with implications for future forecasts.

1. Introduction

The California Current System (CCS) is a highly productive eastern boundary upwelling system that supports numerous commercially important fisheries. However, despite more than seven decades of sustained and ever-expanding measurements in the CCS (Edwards et al., 2010; McClatchie, 2016), we still have a limited understanding of the mechanisms that affect the ecosystem, hindering our ability to forecast biological responses to future ocean changes.

The El Niño-Southern Oscillation (ENSO) cycle is the dominant physical signal across the Pacific Ocean and, in the CCS, generally induces temporary warming, decreased primary production, and enhanced influx of subtropical waters (Ramp et al., 1997; Lynn and

Bograd, 2002; Jacox et al., 2016). El Niño expressions can vary substantially and are now often divided into two types (Kao and Yu, 2009; Capotondi et al., 2015). Eastern Pacific events ('EP Niños') tend to produce strongest changes in the CCS, notably enhanced poleward flow of warm, low-productivity subtropical waters from the south (Ramp et al., 1997; Lynn and Bograd, 2002). The 2015–16 EP Niño produced moderate warming, enhanced poleward transport, and thermocline depression, notably in the southern CCS (Jacox et al., 2016; Rudnick et al., 2017). In contrast, Central Pacific events ('CP Niños') usually produce only weak-to-moderate changes in the CCS (Lilly and Ohman, 2021). The 2009-10 CP Niño depressed the CCS thermocline but did not induce observable changes in circulation (Todd et al., 2011). In addition, an unprecedented Warm Anomaly occurred in the Eastern North Pacific

^{*} Corresponding author. Hatfield Marine Science Center, Oregon State University, 2030 SE Marine Science Drive, Newport, OR, USA, 97365. E-mail address: 11lilly@ucsd.edu (L.E. Lilly).

from spring 2014-summer 2015 (Bond et al., 2015; Zaba and Rudnick, 2016). Although not an El Niño, this event produced extremely warm, stratified, low-nutrient conditions across the southern CCS (Zaba and Rudnick, 2016; Chao et al., 2017; Gentemann et al., 2017; Lilly et al., 2019). Prolonged heat waves are predicted to increase in coming decades (Frolicher et al., 2018; Cheung and Frolicher, 2020), so examining ecosystem responses to past El Niño events and other warm anomalies can help identify underlying forcing mechanisms and predict future ecosystem shifts.

Euphausiids (krill) provide an optimal food web pathway compared to other zooplankton groups (Ruzicka et al., 2012) and comprise significant proportions of the diets of many pelagic fishes, whales, and seabirds (Croll et al., 2005; Ainley and Hyrenbach, 2010; Miller et al., 2010; Santora et al., 2011, 2020; Brodeur et al., 2019). However, some euphausiid species, notably cooler-water and lipid-rich Thysanoessa spinifera (Fisher et al., 2020), provide more optimal prey sources than subtropical species (e.g., Nyctiphanes simplex) that tend to only increase in the southern CCS during El Niño-like perturbations (Brinton, 1981; Lilly and Ohman, 2021). Higher trophic levels in the CCS have been shown to selectively forage on certain lipid-rich euphausiid species even when other euphausiids are more abundant (Daly et al., 2013; Nickels et al., 2018, 2019). Reduced availability of preferred prey can thus alter foraging success or induce prey-switching in higher trophic levels, altering their spatial movements and increasing potential overlap with deleterious human activities (Santora et al., 2020).

Euphausiid species in the southern CCS show clear responses to El Niño events (; Lilly and Ohman, 2018, 2021; Pares-Escobar et al., 2018; Lavaniegos et al., 2019), making them a promising taxon to examine forcing mechanisms of population change. Most euphausiids in the CCS have lifespans of approximately 8 months (*N. simplex*, Lavaniegos, 1992; Gomez, 1995) to 1.5 years (*Euphausia pacifica*, Ross, 1982; Ross et al., 1982) and reach maturity in 3–4 months (Ross et al., 1982). Their spring populations thus tend to be good indicators of the strong winter impacts of El Niño events.

Past studies of euphausiid responses to both short-term El Niño and longer-term decadal perturbations have found evidence for advection into new regions (Dorman et al., 2011; Di Lorenzo and Ohman, 2013) and *in situ* population changes with altered habitat (Pares-Escobar et al., 2018). Both Brinton (1981) and Lilly and Ohman (2021) attributed intrusions of subtropical euphausiids into the southern CCS during El Niño events predominantly to anomalous poleward and shoreward transport but range contractions of resident cool-water species off California conversely to population die-offs and reduced reproduction under unfavorable *in situ* ocean conditions. Various studies have also hypothesized that subtropical species temporarily reproduce in their northward extensions off California under favorable El Niño conditions (Keister et al., 2005; Lilly and Ohman, 2021).

The California Cooperative Oceanic Fisheries Investigations program (CalCOFI) provides sampling coverage of CCS zooplankton nearly unparalleled across the ocean (Edwards et al., 2010) but currently lacks the high temporal resolution to evaluate sub-annual population dynamics, specifically rapid increases indicative of either enhanced advection or reproductive responses to changing habitat conditions. Population modeling provides a complementary tool to examine possible mechanisms of influence in the intervening periods. However, most CCS euphausiid species lack sufficient measurements of growth and reproductive rates to develop individual-based models (IBMs) of population fluctuations (but see Dorman et al., 2011).

This study developed a framework for identifying the extent to which variability in advection alone can explain interannual population fluctuations of six euphausiid species (Euphausia pacifica, Nematoscelis difficilis, Thysanoessa spinifera, Nyctiphanes simplex, Euphausia eximia, Euphausia gibboides) in the southern CCS. We applied a box model assessment, in which we evaluated variability in modeled flow magnitude (supplied by the California State Estimate, CASE, a regionally optimized hindcast adapted from the MITgcm; see Section 2.2) from a

source box encompassing a species' population center to an end box encompassing the sampled CalCOFI region. Due to challenges and complex data requirements for modeling absolute abundance, as well as the limited length (10 years) of our timeseries, we chose instead to examine fluctuations in anomalies of biomass and flow. We hypothesize that, if advection is a significant driver of interannual population change, we will see strong correlations between flow and biomass anomalies.

We focus our study on the 2009-10 CP Niño, 2014-15 Warm Anomaly, and 2015–16 EP Niño in comparison to surrounding non-anomalous years, and specifically ask whether, for each species:

- 1. Can interannual population variability be entirely explained by changes in advection from an upstream "source" region?
- 2. Do the adult and calyptopis larval phases show differential responses to source flow anomalies?
- 3. Do the waters that encompass the spring population have different winter origins during the three anomalously warm years compared to other years?

2. Methods

2.1. Euphausiid collection and enumeration

All euphausiid data come from the California Cooperative Oceanic Fisheries Investigations (CalCOFI) sampling program, which conducts quarterly cruises each year off Central and Southern California. The program samples on a regular station grid (see https://calcofi.org/for complete station map), but the actual subset of stations sampled in a year depends on weather conditions and ship time. Zooplankton are sampled on all cruises but are only enumerated taxonomically from the spring (April/May) cruise (see Lavaniegos and Ohman (2007) and Lilly and Ohman (2018) for complete sampling and preservation procedures). Our timeseries are thus interannual spring biomass values. For each station, an aliquot is sorted and all euphausiids are identified to species level and life-history phase. Body lengths are converted to carbon biomass using known taxon-specific length-carbon relationships (Ross, 1982; Lavaniegos and Ohman, 2007). We considered only nighttime samples to eliminate complications from day/night vertical migration and daytime net avoidance. For the current study, we conducted all calculations using log(carbon biomass (mg C m⁻²)+1) to reduce skew from single values of extremely high biomass.

2.2. CASE model and study region

We used flow fields from the California State Estimate (CASE), a regionally optimized hindcast adapted from the Massachusetts Institute of Technology general circulation model (MITgcm; Marshall et al., 1997) and the Estimating the Circulation and Climate of the Ocean (ECCO; Stammer et al., 2002) four-dimensional variational (4DVAR) assimilation system. The CASE model domain used here encompasses the region between longitudes 114°W-130°W and latitudes 27°N-40°N and is integrated on a (1/16)0 by (1/16)0 spherical polar grid with 72 z-depth levels of varying thickness. The physical data assimilated include profiles from Argo floats (Roemmich et al., 2009), the California Underwater Glider Network (CUGN, Rudnick et al., 2017), and expendable bathythermographs (NOAA, 2021). The resulting flow fields are validated against the CalCOFI hydrography dataset. See Zaba et al. (2018) for more information about model data assimilation and forcing. We used daily-averaged currents from 38 non-overlapping three-month hindcasts between 1 October 2007-31 March 2017.

2.3. Flow-biomass anomalies and source boxes

2.3.1. Biomass anomalies

We analyzed six euphausiid species, categorized as either 'cool-

water' (Euphausia pacifica, Nematoscelis difficilis, Thysanoessa spinifera) or 'subtropical' (Nyctiphanes simplex, Euphausia eximia, Euphausia gibboides) based on previously described biogeographic distributions (Brinton, 1962; Lilly and Ohman, 2021). For each species at each station, we first calculated the ten-year timeseries of biomass anomalies (2008–2017) by subtracting that station's ten-year mean from each yearly value. We then computed a spatially-averaged anomaly for each year by averaging all of the station-specific biomass anomalies from that year for a given species. Since each year contains a different subset of CalCOFI stations, years with zero total biomass can have slightly different negative anomalies. We noted years of zero biomass for N. simplex, E. eximia, and E. gibboides with asterisks ('*') on the x-axes in Fig. 3 to distinguish them from non-zero negative biomass anomalies.

2.3.2. Flow anomalies

For both the flow-biomass comparisons (Section 2.3.3) and particle backtracks (Section 2.4), we integrated the u (x-directional velocity) and ν (y-directional velocity) flow fields (both as m/s) separately for 0–150 m depth (encompassing 15 flow levels, where each level encapsulates 10 m depth). We chose this depth range to encompass the nighttime vertical distributions of the species analyzed here (Brinton, 1962; Matthews et al., 2020). To calculate anomalies in each flow field, we first removed an interannual mean (2008-2017) and seasonal cycle from each grid point in the flow field, separately for the u and v fields. For each month in the timeseries (separately for each year), we calculated an average flow field from all daily anomalies within that month. We then applied a 2D Gaussian smoothing filter to the flow fields to remove fine-scale variability (Von Storch and Zwiers, 2002). The filter had a standard deviation of 60 km (isotropic in x and y), with influence truncated beyond 5x the standard deviation (300 km total). All flow values within that range (150 km on either side of the center flow point) were averaged using their Gaussian weights (i.e., flow values farthest away had the smallest weights) to produce a weighted-average value at that point. Flow anomalies for flow-biomass correlations (Section 2.3.3) were calculated from the filtered flow fields, but particle backtracks (Section 2.4) used the unfiltered flow fields.

2.3.3. Source boxes and flow-biomass correlations

For each species, we defined a 'flow source box' to encapsulate the portion of the flow field that connects that species' highest average population center (previously defined by Brinton, 1962; Lilly and Ohman, 2021) to the CalCOFI sampling region off Southern California (Fig. 1; white boxes indicate highest average population centers). Each

source box has an associated compass direction of flow that represents the expected dominant straight-line path from the highest-population center into the lower-population CalCOFI sampling region (Fig. 2).

For each species, we lag-correlated the filtered flow in the specified direction averaged within the source box with the corresponding spring biomass anomaly for that year. Correlations compared the spring biomass anomaly to monthly-averaged time-lagged flow magnitude for each of the preceding 1–5 months (November–March). We calculated correlations for total population, adult (fully mature), and calyptopis (newly reproduced) biomass anomalies for each species. Total biomass also includes the furcilia and juvenile stages, which were not analyzed individually in this study. Calyptopis correlations for $\it E. eximia$ and $\it E. gibboides$ used abundance (no. m $^{-2}$) because mean biomass was effectively zero due to small body size and sparse presence.

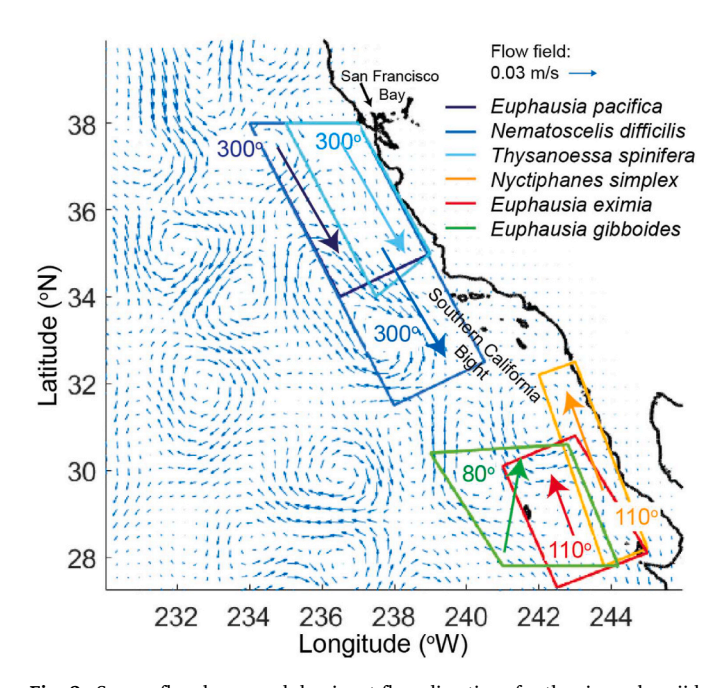


Fig. 2. Source flow boxes and dominant flow directions for the six euphausiid species, as shown in Fig. 1. Flow directions are labeled in degrees next to each arrow. Boxes and arrows are overlaid onto monthly average flow for March 2008. Labels ('San Francisco Bay', 'Southern California Bight') indicate geographic locations referenced in this study.

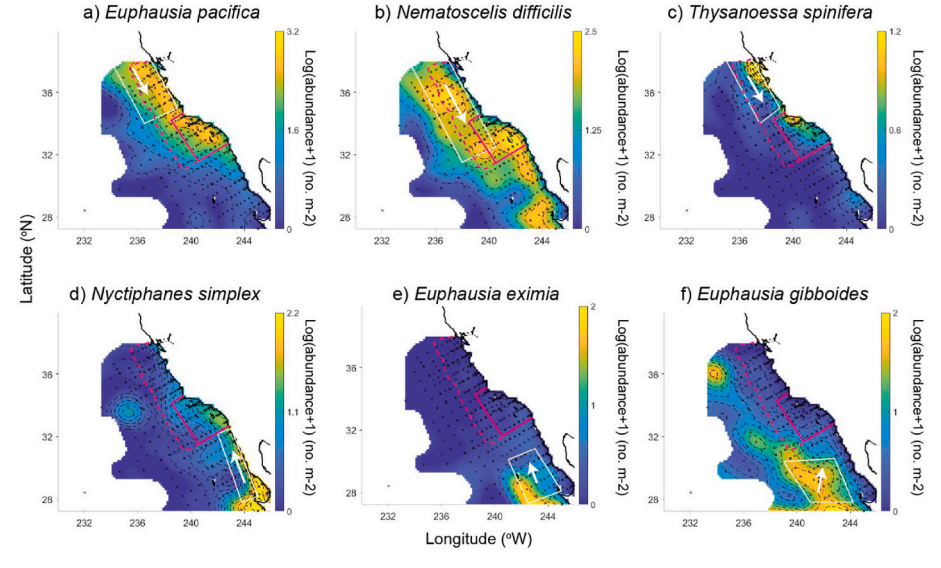


Fig. 1. Average spring distribution of each euphausiid species (1951–2018), objectively mapped from CalCOFI samples (maps are reproduced from Lilly and Ohman (2021); black crosses indicate CalCOFI stations). White boxes and arrows indicate the source flow box and dominant flow direction assigned to each species used to calculate Figs. 3–5 (see Section 2.3.3). Pink boxes show the core CalCOFI sampling region (solid pink rectangle) and additional CalCOFI region sampled in some years (dashed pink region).

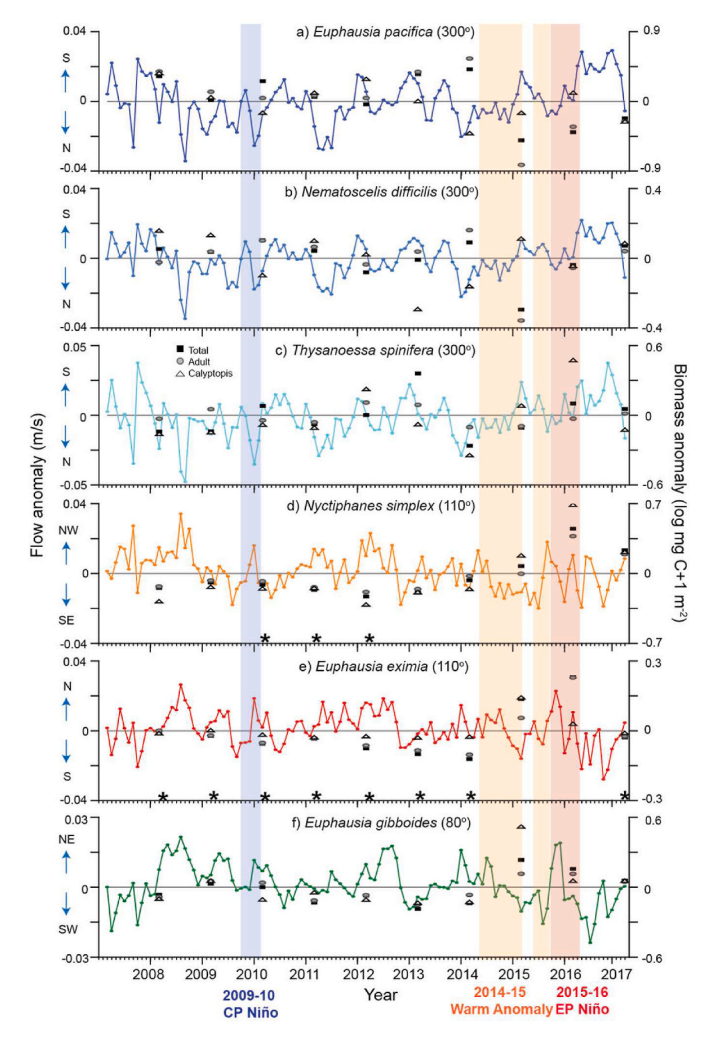


Fig. 3. Flow timeseries (lines) from the source box and dominant flow direction defined for each species (see Fig. 1 and 2), and corresponding species spring regionwide average biomass anomalies (symbols). Flow timeseries are calculated at monthly average timesteps, and only include the component in the defined dominant flow direction (indicated by degree values after species name). Arrows and cardinal directions next to left axes indicate flow directions corresponding to positive and negative flow anomalies. Biomass symbols: Total – black squares; Adult – grey circles; Calyptopis – white triangles. Calyptopis stages of *E. eximia* and *E. gibboides* are for abundance (log no. m⁻²). Black asterisks ('*') on x-axes indicate years of zero biomass (no presence) for a species, to differentiate from years of non-zero negative biomass anomalies. Shaded vertical bars indicate the temporal extents of 2009–10 CP Niño (purple), 2014-15 Warm Anomaly (orange), and 2015–16 EP Niño (red). The Warm Anomaly diminished in spring 2015 and reappeared in summer (second orange shaded bar), immediately prior to the 2015–16 El Niño.

2.4. Particle-tracking model

2.4.1. Model setup

To estimate winter origins of the water mass that encompassed each euphausiid spring distribution, we backtracked a particle-tracking model forced by the CASE u and v flow fields (see Section 2.3.2 for explanation) from 31 March to the prior 1 December for each year (fourmonth span; see Fig. 6 for example backtracks). We again used the flow fields integrated from 0 to 150 m depth, although here we used the unfiltered fields. Our particle-tracking model interpolates gridded velocities to particle positions using an integration timestep of 0.01 day (100 timesteps for each 24-hr flow point) using the Runge-Kutta method, a standard method for the accurate numerical integration of ordinary differential equations and which has higher accuracy than

simple forward integration (Butcher, 1987). New three-month trajectories of the flow fields begin each 1 January, creating potential discontinuity with the previous 31 December, but the integrative nature of the particle-tracking model reduced any impacts of discontinuities on the trajectories. We compared forward (1 December to 31 March) and backward (31 March to 1 December) trajectories of the same particle and found $<\!10^{-6}$ m displacement between the original 1 December starting location and resulting 1 December backtrack endpoint, indicating that integration does not significantly bias the tracks.

To determine whether small displacements in the seeding locations of particles produced substantially different end-locations, we calculated the 'end-spreads' between groups of 25 particles seeded within 0.1° , 0.05° , or 0.01° grid cells. In almost all cases, the end-spread between particles from the 0.1° grid cell was $<0.2^{\circ}$ in x and y, which was sufficient to depict the larger-scale resolution of water parcel circulation in which we were interested. We also tested the addition of random diffusivity values to the u and v flows at each timestep, where the diffusivity values were drawn from a random distribution with mean = 0 and S.D. = 0.02 m/s. We observed deviations of <50 km between the end-locations of particles influenced by random diffusivity and those without diffusivity, which was sufficiently small in the context of the large-scale processes we focused on for this study. We thus chose to run the particle backtracks without a diffusivity component.

2.4.2. Particle seeding for backtracks

For each species, we seeded particles on 31 March in the regions of $>\!50\%$ and $>\!80\%$ of the maximum biomass of that year (e.g., if the maximum biomass in the distribution for a year was $1.0\log\,[\mathrm{mg}\,\mathrm{G}\,\mathrm{m}^{-2}]$, any region with at least $0.8\log\,[\mathrm{mg}\,\mathrm{G}\,\mathrm{m}^{-2}]$ was encompassed by the 80% contour). We determined these regions by first objectively mapping all stations from an individual spring into a smoothed regionwide distribution (Lilly and Ohman, 2021) and then calculating the 50% and 80% biomass contours on that map. We specified and color-coded the 50% and 80% regions separately to determine whether regions of higher biomass were affected by different proportions of a water mass, although we used the same particle-seeding concentration for both regions.

We seeded particles for the three anomalous springs (2010, 2015, 2016; see Fig. 6) at resolutions of one particle per 0.13° latitude and 0.16° longitude spacing (100 particles each in the full latitude and longitude ranges of CASE, i.e., a 100×100 particle grid across the model region). For all non-Niño years for a species, we created one composite backtrack. First, for each individual year, we seeded 20 particles per latitude and longitude ranges (0.65° latitude and 0.8° longitude spacings) for *E. pacifica* and *N. difficilis*, or 50 particles (0.26° and 0.32° , respectively) for the other four species. We used lower concentrations for *E. pacifica* and *N. difficilis* to visually offset their higher population levels. Second, we calculated the composite non-Niño spring distribution for a species by averaging all years of biomass by station, then objectively mapping the average distribution and identifying its 80% and 50% thresholds.

2.4.3. Quantifying particle end-locations

We calculated the proportions of winter backtracked particles that ended in each of four quadrants depicting major hydrographic regions of the CCS, plus a fifth category of particles originating outside the model region (Fig. 12): Q1 – Northern Inshore, including coastal central California and inshore California Current (CC); Q2 – Northern Offshore, including offshore CC and northern North Pacific Central Gyre; Q3 – Southern Offshore, dominated by the North Pacific Central Gyre and encompassing the outer southern CC; Q4 – Southern California Bight south of Pt. Conception to northern Baja California, including the inshore portion of the southern CC; Q5 – area outside the CASE domain. Particle proportions were calculated for each year as the number of particles in that quadrant divided by the total number of particles initially seeded across both the >50% and >80% regions. Particle

proportions for all species were calculated using 50 particles per latitude and longitude ranges, as described in Section 2.4.2.

3. Results

3.1. Timeseries of source box flow and biomass

3.1.1. Cool-water species

The *E. pacifica* source box showed periods of notable negative (reduced southward or possible northward) flow anomalies in Sep 2007, Sep 2008, Jan 2010, Jun–Aug 2011, and Jan 2014 (Fig. 3a). Moderate negative flow anomalies occurred during parts of the Warm Anomaly (Oct–Dec 2014) and 2015–16 EP Niño (Oct 2015–Jan 2016). In contrast, strongly positive (southward) flow anomalies occurred in Jan 2008, Mar–May 2015, and Apr 2016–Feb 2017. Total and adult spring biomass of *E. pacifica* were moderately positive in 2010, highest in 2014, and lowest in 2015 and 2016 (Fig. 3a, black squares and grey circles for total and adult, respectively). Calyptopis (larval) biomass shows the opposite pattern, with highest anomalies coincident with years of high spring flow, and most negative biomass in 2014 but increasing sequentially through 2015 and 2016 (Fig. 3a, white triangles).

The source box for *N. difficilis* encompasses an overlapping, though larger, region compared to *E. pacifica*, so its flow timeseries showed similar but smaller-magnitude anomalies due to the larger averaging region (Fig. 3b). Total and adult biomass anomalies were high in 2014, low in 2015, and neutral in 2016, while calyptopis biomass was low in 2013 and 2014 but high in 2015. Flow anomalies for *T. spinifera* had more month-to-month variability than for the other cool-water species but showed clear negative anomalies in winter 2009–10, during the CP Niño (Fig. 3c). Total biomass of *T. spinifera* was anomalously elevated in spring 2013 and low in spring 2014. Positive calyptopis biomass anomalies in 2012 and 2016 and negative anomalies in 2014 and 2017 coincided with positive or negative spring flow anomalies, respectively.

3.1.2. Subtropical and tropical species

Source box flow for *N. simplex* showed periods of moderate positive (poleward) flow anomalies during the 2009-10 CP and 2015-16 EP Niños but negative (equatorward) flow throughout most of the 2014-15 Warm Anomaly (Fig. 3d). Calyptopis biomass anomalies of N. simplex tracked adult and total populations across all years; N. simplex calvptopes were not detected in the CalCOFI region in 2010-2012 (Fig. 3d, asterisks denote zero-biomass years). The flow timeseries for E. eximia showed similar poleward anomalies as for N. simplex during the 2009-10 CP Niño; however, during the 2014-15 Warm Anomaly, the E. eximia source region had a more pronounced period of northward flow, while during 2015-16 it showed later onset of enhanced northward flow compared to N. simplex (Fig. 3e). Euphausia eximia was only detected in the CalCOFI region in springs 2015 and 2016; calyptopis anomalies were higher in 2015, while total and adult populations were higher in 2016. The flow timeseries of E. gibboides similarly showed moderately enhanced poleward/onshore flow at the end of the 2009-10 CP Niño and strongly enhanced poleward/onshore flow at the beginning of the 2015-16 EP Niño, aligned with E. eximia (Fig. 3f). Total population biomass of E. gibboides was correspondingly highest in spring 2015 and moderately elevated in spring 2016; calyptopis biomass was notably high in 2015.

3.2. Time-lagged correlations of flow versus biomass

To examine potential co-variability of euphausiid biomass with source flow, we calculated time-lagged correlations between spring biomass anomalies (April–May) and the preceding five months of flow anomalies (November–March) for each species (Fig. 4). Comparisons of biomass with flow from 6 to 10 months prior yielded only weak correlations, so we did not include them in our analyses (data not shown; $|\mathbf{r}| < 0.50$, p > 0.15). Euphausia pacifica and N. difficilis biomasses correlated

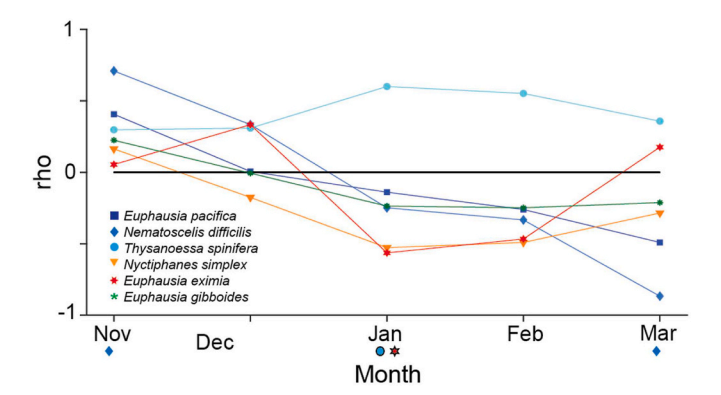


Fig. 4. Correlations of euphausiid spring biomass with flow anomalies from November–March. Biomass is the total for each species (black squares in Fig. 3). Both flow and biomass were spatially averaged across their respective regions before correlating; flow anomalies were additionally averaged within a month. Blue diamonds below x-axis denote significant correlations of *Nematoscelis difficilis* with Nov and Mar flows (p < 0.05); blue circle and red star below 'Jan' denote borderline significant correlations (p < 0.10) for *T. spinifera* and *E. eximia*, respectively.

most positively with November source flows (Fig. 4; r=0.41 and r=0.71 for *E. pacifica* and *N. difficilis*, respectively; p<0.05 for *N. difficilis*). November flow can thus explain >50% of population variability in *N. difficilis*. Correlations declined steadily to strongest negative values in March (r=-0.49 and -0.87 for *E. pacifica* and *N. difficilis*, respectively; p<0.05 for *N. difficilis*). March flow thus explains >75% of population variability in *N. difficilis*. In contrast, *T. spinifera* showed increasingly positive correlations with flow through January (r=0.60, p<0.10) and remained strongly positive through March (Fig. 4). January flow can thus explain 36% of *T. spinifera* variability.

Nyctiphanes simplex and E. gibboides showed similar correlation patterns to E. pacifica and N. difficilis from November–January, although N. simplex had weaker positive and stronger negative correlations throughout (Fig. 4). Unlike the two cool-water species, however, N. simplex showed a slight increase and E. gibboides maintained near-constant values for February–March correlations. In contrast to all other species, E. eximia showed highest positive correlation with flow in December, followed by strongest negative correlation in January (r = -0.56, p < 0.10), before again returning to a positive correlation with March flow (Fig. 4). January flow can thus explain 35% of E. eximia variability.

We also examined separate adult and calyptopis time-lagged correlations with flow to determine whether different developmental phases responded similarly (Fig. 5). The three cool-water species showed opposite correlation patterns for adult and calyptopis phases (Fig. 5a–c). Adult patterns tracked correlations for total biomass, as expected, with *N. difficilis* adults correlating significantly negatively with March flow (r = -0.80, p < 0.01). In contrast, all three species showed increasingly positive calyptopis correlations throughout parts of January–March, with *T. spinifera* correlating significantly positively with March flow (r = 0.78, p < 0.05). In notable contrast, all three subtropical species showed consistent correlation patterns across the adult and calyptopis phases (Fig. 5d–f). Calyptopis biomass for *N. simplex* showed a significant

negative correlation with January flow ($r=-0.78,\,p<0.05$). More than 60% of the fluctuations of these three species-phases can thus be explained by their associations with horizontal flows.

3.3. Particle tracking to determine winter origins of source waters

Particle backtracks from 31 Mar to the previous 1 Dec of each year revealed the winter origins of the water masses encompassing each species in spring, as well as the possible winter origins of the spring populations themselves.

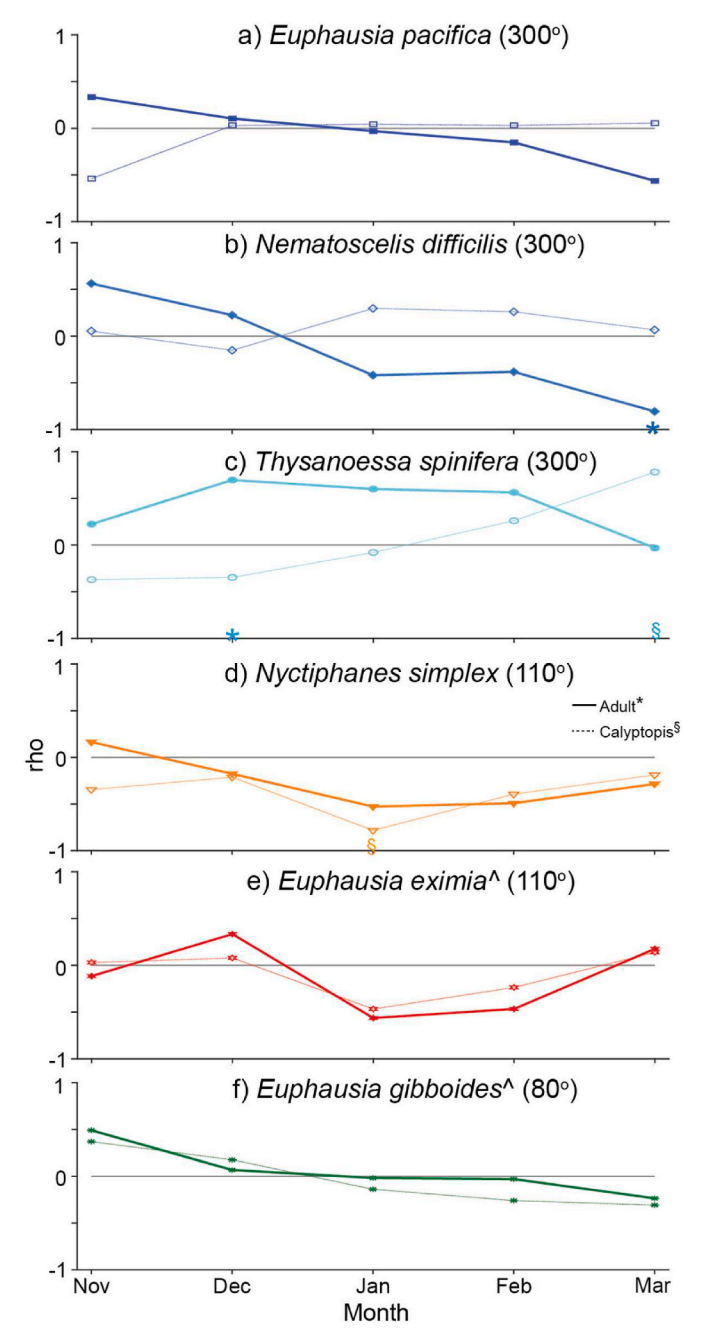


Fig. 5. As in Fig. 4, but for adult (solid lines, filled symbols) and calyptopis larvae (dashed lines, open symbols) spring biomasses versus flow anomalies. Symbols indicate significant correlations (p < 0.05): *adult, \S calyptopis. *Euphausia eximia* and *E. gibboides* calyptopis correlations are for abundance (log no. m $^{-2}$).

3.3.1. Cool-water species

Spring distributions of *E. pacifica* showed shoreward compression in all three anomalous years and northward shifts and reduced maximum biomass areas in 2015 and 2016 compared to the non-Niño composite (Fig. 6, pink dashed and solid lines). Winter particle origins for 2009–10 and 2015-16 did not come from as far offshore in the southern part of the model domain (south of 34° N) as in the non-Niño composite; winter origins for the 2014-15 Warm Anomaly included one offshore tendril but almost no waters south of 31° N (Fig. 6b–d, blue and turquoise symbols; see https://doi.org/10.6075/J0KK9BZP for animations of daily-resolution particle backtracks for each species and year).

Nematoscelis difficilis showed slightly shoreward contraction of its

spring distribution during the 2014-15 Warm Anomaly compared to the non-Niño composite, but no notable changes during the other two anomalies (Fig. 7, pink dashed and solid lines). Similarly, winter origins of *N. difficilis* during 2014–15 did not extend as far offshore in the southern region (south of 32°N) as during other years (Fig. 7c, blue and turquoise symbols; https://doi.org/10.6075/JOKK9BZP for animated yearly backtracks). *Thysanoessa spinifera* did

not show reduced spring distributions during any anomalous year (Fig. 8, pink dashed and solid lines). However, its winter origins during the 2014-15 Warm Anomaly had an offshore tendril but were mostly confined north of 31°N, as for *E. pacifica* (Fig. 8c, blue and turquoise symbols; see https://doi.org/10.6075/JOKK9BZP for animated yearly backtracks). Winter origins of *T.spinifera* during the 2015–16 EP Niño showed low numbers of particles within the CASE region compared to other years, despite a similar spring distribution (Fig. 8d).

3.3.2. Subtropical species

The non-Niño average spring distribution of *N. simplex* shows high biomass only at San Francisco Bay, CA (Fig. 9a, 37.5°N; see Fig. 2 for location of San Francisco Bay), but this is an aberration caused by two high-biomass points dominating the overall non-Niño average.

However, backtracks for the non-Niño composite were run for each year separately, so they represent the true compilation of winter source waters across those years. The very low population average for the non-Niño composite of *N. simplex* makes it difficult to compare distributional changes in 2014–15 and 2015–16, but during 2014–15 they were shifted notably more northward than in 2015–16 (Fig. 9c–d). Winter source waters in 2014–15 contained some of the farthest northward and offshore origins of all years; in contrast, source waters for 2015–16 originated closer inshore and farther south (Fig. 9, blue and turquoise symbols; see https://doi.org/10.6075/JOKK9BZP for animated yearly backtracks).

Euphausia eximia was only detected in the CalCOFI region in springs 2015 and 2016, so we cannot compare those distributions to non-Niño years. However, spring 2015 showed a farther northward population extension than did spring 2016 (Fig. 10c-d, pink dashed and solid lines). Winter source waters in 2014-15 also contained more northern and offshore origins, while source waters for 2016 originated mostly within the SCB (Fig. 10c-d, blue and turquoise symbols; see https://doi. org/10.6075/J0KK9BZP for animated yearly backtracks). In contrast, E. gibboides showed a consistent offshore presence throughout both non-Niño and anomalous years, although it extended notably shoreward in spring 2015 and moderately in spring 2016 (Fig. 11, pink dashed and solid lines). Winter source waters again show greater offshore origins during 2014-15 compared to the other anomalous years, while 2015-16 had higher origins nearshore off California (Fig. 11c-d, blue and turquoise symbols; see https://doi.org/10.6075/J0KK9BZP for animated yearly backtracks).

3.3.3. Particle backtracks by quadrant

Quantification of particle endpoints in the four quadrants of the CASE region (Fig. 12; see Section 2.4.3) showed that winter source waters for E. pacifica originated fairly equally across the model domain, with generally highest contributions from northern offshore (Q2) waters (Fig. 13a). However, all three anomalous events had some of the lowest contributions from the southern offshore (Q3) and southern nearshore (Q4) regions, particularly for 2015-16. The 2009-10 event had the highest source water contributions from Q2 of any year, while 2015-16 had the highest source water contribution of any year from the northern inshore region (Q1). Nematoscelis difficilis had notable contributions during 2014-15 from both northern and southern offshore regions (Fig. 13b, Q2 and Q3, yellow triangles). In contrast, the other two anomalous years had among the lowest contributions from southern offshore and nearshore waters for N. difficilis, although 2015-16 again had the highest contribution of any year from northern nearshore waters (Fig. 13b, red triangle). Thysanoessa spinifera showed highest

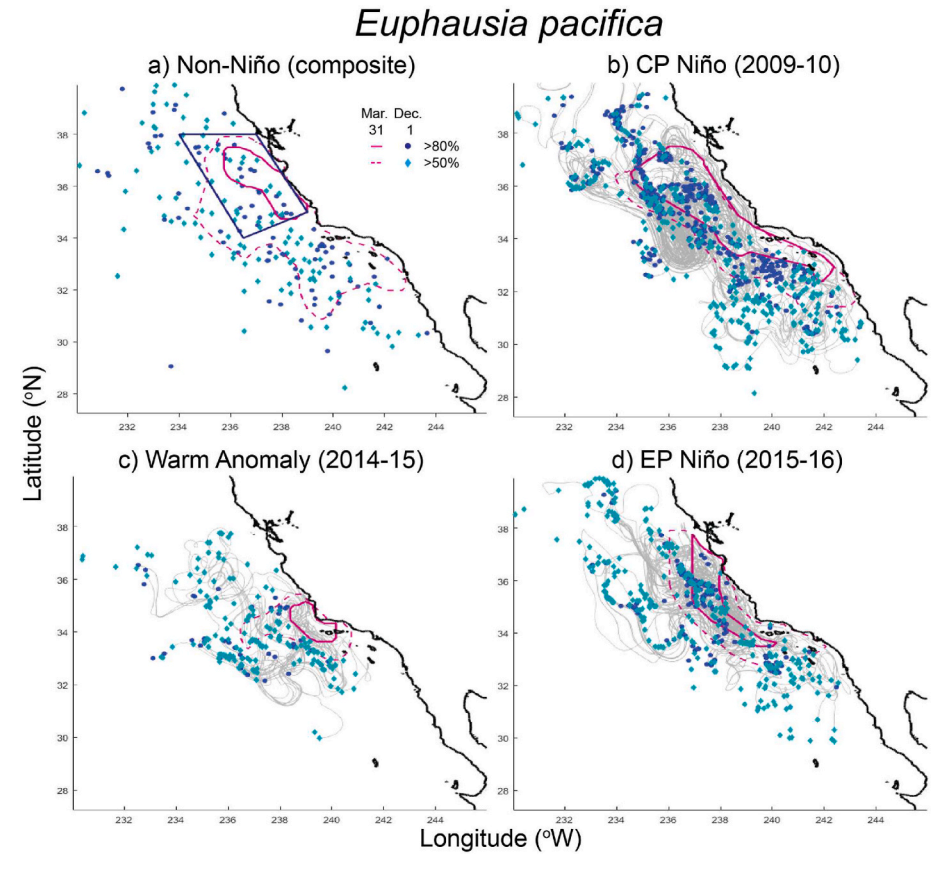


Fig. 6. December 1 particle locations indicating winter origins of Euphausia pacifica particles backtracked from March 31 for: a) the seven non-Niño years from 2008 to 2017 (all years composited), b) 2009-10 CP Niño, c) 2014-15 Warm Anomaly, and d) 2015-16 EP Niño. Pink lines indicate the 50% (dashed) and 80% (solid) contours of the population for a given spring, except panel 'a' shows the average distribution across the seven non-Niño springs (see Section 2.4.2). Particles were seeded within these regions on March 31; dark blue symbols indicate backtrack endpoints from the 80% region, turquoise symbols indicate the 50% region. Grey lines show backtrack paths (only shown for every fifth particle for this species). For each composite year, only 20 particles were seeded per latitude and longitude ranges (20 \times 20 particle grid), as opposed to 100 \times 100 for individual years, to improve visualization. Blue polygon in panel 'a' is the source flow box for E. pacifica.

Nematoscelis difficilis

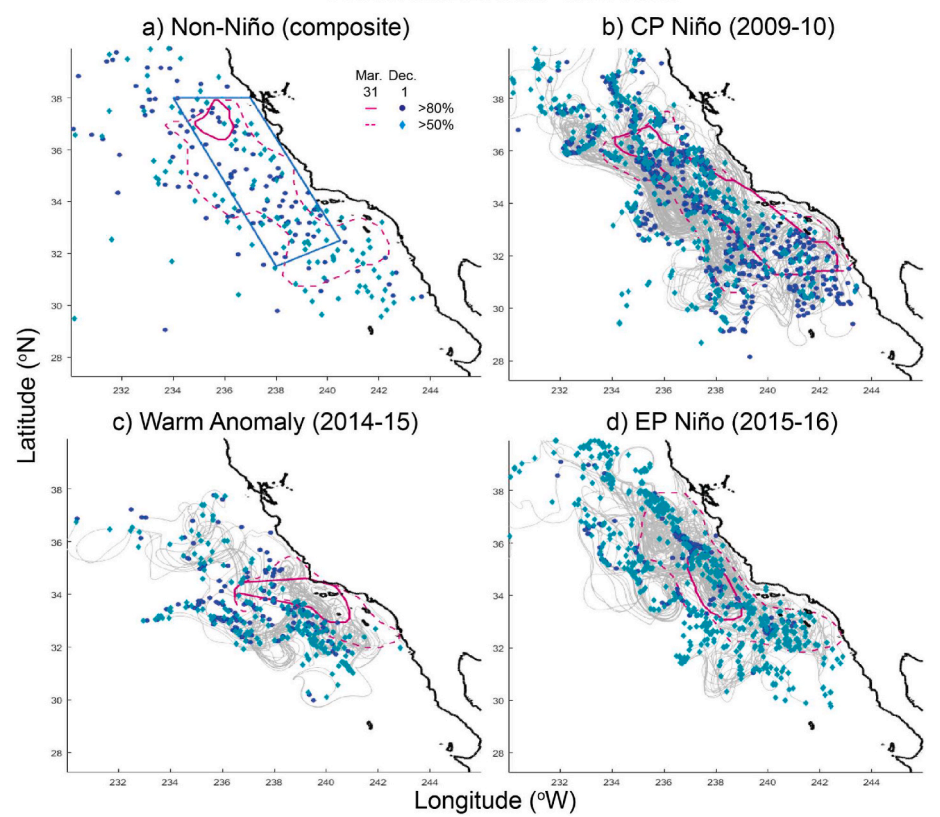


Fig. 7. As in Fig. 6, but for Nematoscelis difficilis. Particle backtrack lines are only shown for every fifth particle.

Thysanoessa spinifera a) Non-Niño (composite) b) CP Niño (2009-10) Mar. Dec. 31 1 280% 36 20 202 234 236 238 240 242 244 c) Warm Anomaly (2014-15) d) EP Niño (2015-16)

Fig. 8. As in Fig. 6, but for *Thysanoessa spinifera*. Particle backtrack lines are only shown for every fifth particle. For the composite non-Niño plot (panel 'a'), each year was seeded with a 50×50 particle grid.

contributions of particles from outside the model domain (Q5) across most years, particularly in 2015–16 when nearly 80% of particles originated outside the model domain (Fig. 13c). In contrast, 2009-10 had the second highest contributions from northern nearshore waters (Q2). As for the other cool-water species, *T. spinifera* showed among the lowest contributions from Q3 and Q4 in 2015–16.

Nyctiphanes simplex also showed overall highest contributions from outside the model domain (Q5), particularly during 2015–16 (Fig. 13d; N. simplex was absent in three years, including 2009–10). The 2014-15 event had its highest contribution from northern offshore waters (Q2), and both 2014–15 and 2015-16 had high contributions from the southern nearshore region (Q4) compared to non-Niño years. Euphausia eximia was only present in 2014–15 and 2015–16; its source waters appeared to originate mostly from Q4 in 2014–15, and equally from the southern regions and outside the model domain in 2015–16 (Fig. 13e). Euphausia gibboides showed highest source water contributions of any species from the northern offshore region (Q2), although lower during the three anomalous events compared to non-Niño years (Fig. 13f). Both 2009–10 and 2015-16 had among the highest contributions from northern nearshore waters (Q1), while 2014–15 was the year most strongly influenced by offshore southern waters (Q3).

4. Discussion

By definition, predominantly passive zooplanktonic organisms experience a strong influence of advection on their movements and distributions. The present study examined the extent to which advection alone explains interannual variability in six euphausiid species in the southern California Current System, as well as whether cool-water species (Euphausia pacifica, Nematoscelis difficilis, Thysanoessa spinifera) and subtropical species (Nyctiphanes simplex, Euphausia eximia,

Euphausia gibboides) respond differently to anomalous conditions associated with El Niño-like events.

We found, first, that advection alone does not entirely explain interannual population variability of any of the species considered, although some months do explain high proportions of cool-water species fluctuations. Second, cool-water species show opposite adult and calyptopis correlations with winter-to-spring flow, indicating a mechanism of in situ calyptopis production independent of adult population size. In contrast, subtropical species show consistent flow correlations across adults and calyptopes, indicating whole-population advection into the Southern California Bight. Third, cool-water species inhabited lower proportions of southern-origin waters during the 2014-15 Warm Anomaly and 2015-16 El Niño compared to non-anomalous years, while subtropical species experienced enhanced influence of southern waters. Differential cool-water and subtropical species responses suggest that resident cool-water species are impacted by variability in advection predominantly via altered in situ reproduction of existing populations. In contrast, non-resident subtropical species undergo whole-population transport into the Southern California Bight (SCB). We discuss the reasoning and implications of these inferences below.

4.1. Can advection alone explain population variability?

Significant correlations of N. difficilis with both November (positive) and March (negative) flows and both T. spinifera (positive) and E. eximia (negative) with January flow emphasize that certain months of advection can account for large portions of the interannual fluctuations in these populations (greater than 50% for N. difficilis; \sim 35% for T. spinifera and E. eximia). However, substantially weaker correlation values across most months, and notably all months for E. pacifica and E. gibboides, indicate that neither cool-water nor subtropical species are

Fig. 9. As in Fig. 6, but for *Nyctiphanes simplex*. Particle backtrack lines are show for every particle. Particles for the composite non-Niño were seeded using a 50×50 particle grid. *Nyctiphanes simplex* was not detected in springs 2010, 2011, or 2012; panel 'a' therefore only includes five years, and there is no backtrack for panel 'b'.

Longitude (°W)

simply transported into or out of the SCB every time the currents flow favorably.

The lack of strong correlations of subtropical species with flow, and their increases in the SCB only in springs 2015 and 2016 despite other periods of favorable flow, complicate the hypothesis that subtropical and offshore species increase in the SCB in direct response to anomalous advection (Brinton, 1981; Lilly and Ohman, 2021). Several factors may explain why subtropical species do not always increase during periods of favorable flow: i) the subtropical source water boxes we defined may not extend far enough south or offshore to reach true population centers for these species, ii) enhanced flows may not persist long enough to transport seed organisms all the way to the SCB, or iii) subtropical populations may be transported to the SCB but cannot survive its conditions. Other factors must therefore influence both cool-water and subtropical species, such as in situ reproduction or thresholds of advection that must be surpassed for population increases to occur in the SCB. Although we did not measure these factors, below we examine possible explanations based on differential responses of adult and calyptopis phases of each species.

4.2. Adult and calyptopis phase correlations with flow

4.2.1. Cool-water species: in situ calyptopis production in response to favorable source waters

Spring increases in adult biomass of cool-water species may result from enhanced winter source water advection in different ways. The first is that stronger southward winter flows may transport seed populations of cool-water species from northern higher-biomass regions (Brinton, 1962; Lilly and Ohman, 2021). Given that *E. pacifica* shows an average developmental duration of four months from larval to late juveniles (Ross, 1981), any larval calyptopes transported in winter would develop

to adults by spring, thus adding to spring adult, rather than calyptopis, biomass. A second mechanism is that enhanced southward winter advection transports greater amounts of northern-origin waters, presumably characterized by favorable cool temperatures and high productivity, which could support increased *in situ* winter reproduction of existing cool-water populations off central and southern California (Feinberg and Peterson, 2003; Schroeder et al., 2014; Cimino et al., 2020), also producing calyptopes that would develop to adults by spring. We cannot currently distinguish which of these two mechanisms dominates; both likely contribute to increases in adult populations, dependent on year-specific physical conditions.

In contrast to adults, increases in spring calyptopis biomass of coolwater species must occur differently, since winter-spawned calvptopes will develop to adults by spring. One possibility is that entire seed populations of cool-water species are advected to central and southern California in spring with enhanced southward transport. However, we would expect to see concurrent increases in adults and calyptopes during years of enhanced spring flow, rather than only increases in spring calyptopes during years of reduced adult populations. A second possibility is that existing adult populations of cool-water species reproduce in situ during years of favorable spring-onset conditions, even when the adult populations themselves are low. Both E. pacifica and N. difficilis have been hypothesized to rely on nearshore spawning off central California to maintain population levels in the region (Brinton, 1962), so we expect elevated reproduction to occur in this region whenever habitat conditions become favorable. Rapid re-emergence of reproduction during favorable conditions reiterates that, although dominant zooplankton species often decrease substantially during El Niño, they show long-term reproductive and population resilience to such anomalous events (Lilly and Ohman, 2018, 2021; Lindegren et al., 2018).

The different correlation pattern of T. spinifera with flow compared

Euphausia eximia

a) Non-Niño (composite)

b) CP Niño (2009-10)

No presence

No presence

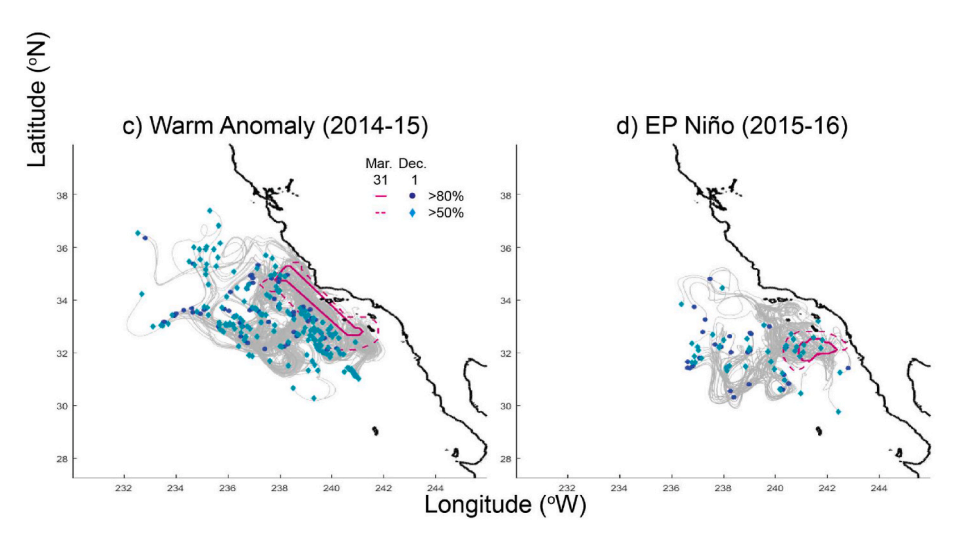


Fig. 10. As in Fig. 9, but for Euphausia eximia. Euphausia eximia was only detected in springs 2015 and 2016.

to the other two cool-water species reflects its higher proportions of calyptopes relative to adults (Brinton, 1962; Lilly and Ohman, 2021). However, elevated total population biomass of *T. spinifera* in some years that produce relatively low biomass of other cool-water species (e.g., 2013), combined with the finding that high proportions of its source waters come from outside our model domain, indicate this species is impacted by additional processes, likely coastal upwelling (Cimino et al., 2020).

4.2.2. Subtropical species: whole-population transport with favorable advection

In contrast to cool-water species, subtropical species show greater consistency of flow correlations across the adult and calyptopis phases, rather than years of only adult or only calyptopis increases. Since we do not observe calyptopis-only increases indicative of spring reproduction, we suggest that subtropical species are influenced by advection primarily via transport of entire populations into the SCB. All three of the subtropical species examined here have average biogeographic distributions in waters to the south (*N. simplex, E. eximia*) or offshore (*E. gibboides*) of California (Brinton, 1962; Lilly and Ohman, 2021), so we expect some requirement of initial advection to seed higher population biomasses into the SCB. The additional positive (albeit low) correlation of *E. eximia* spring populations with March flow suggests that this species, in particular, may undergo secondary spring transport into the SCB.

However, *N. simplex* has been observed to reproduce *in situ* far poleward of its usual habitat ranges during anomalous events such as El Niño (Keister et al., 2005). Populations of *N. simplex* also persist in the SCB at decadal-length scales (Brinton and Townsend, 2003) and related to the influence of the Pacific Decadal Oscillation (Di Lorenzo and Ohman, 2013), rather than simply intruding during El Niño events. Thus, a species such as *N. simplex*, which inhabits a more northerly

extent than *E. eximia*, has likely adapted some ability to reproduce in the SCB during anomalously favorable conditions.

4.3. Differential source water origins during anomalous events

Decreased proportions of cool-water species in southern nearshore and offshore waters during all three anomalous events (2009–10, 2014–15, 2015–16) further support our hypothesis that cool-water species respond to unfavorable El Niño conditions via reduced *in situ* reproduction or population die-offs. Lower associations of cool-water species with southern waters likely reflect reduced population presence – survival and/or reproduction – in these warmer, lower-productivity, and presumably unfavorable waters. This pattern is not always true: all three cool-water species had among their highest associations with southern offshore waters during the Warm Anomaly. Overall, however, cool-water populations were reduced in southernorigin waters during all three events, particularly the 2015–16 EP Niño.

In contrast, subtropical species show enhanced associations with southern waters, either nearshore (*N. simplex*) or offshore (*E. gibboides*), during anomalous events. High contributions of southern nearshore waters to *N. simplex* populations during the 2015–16 EP Niño suggest these waters are particularly favorable for survival, and perhaps even *in situ* reproduction, associated with warmer temperatures (Lilly and Ohman, 2021). The higher associations of *E. gibboides* with southern offshore waters during the three anomalous events aligns with its general biogeographic affinity for offshore Central Gyre waters (Brinton, 1962; Lilly and Ohman, 2021). If subtropical population levels changed solely with variations in source water advection, we would expect the proportions of tracer particle contributions to remain the same across years, with only overall biomass levels varying. Changes in the actual proportions of different source water contributions suggest some component of varying influence on populations, perhaps via *in situ*

Euphausia gibboides

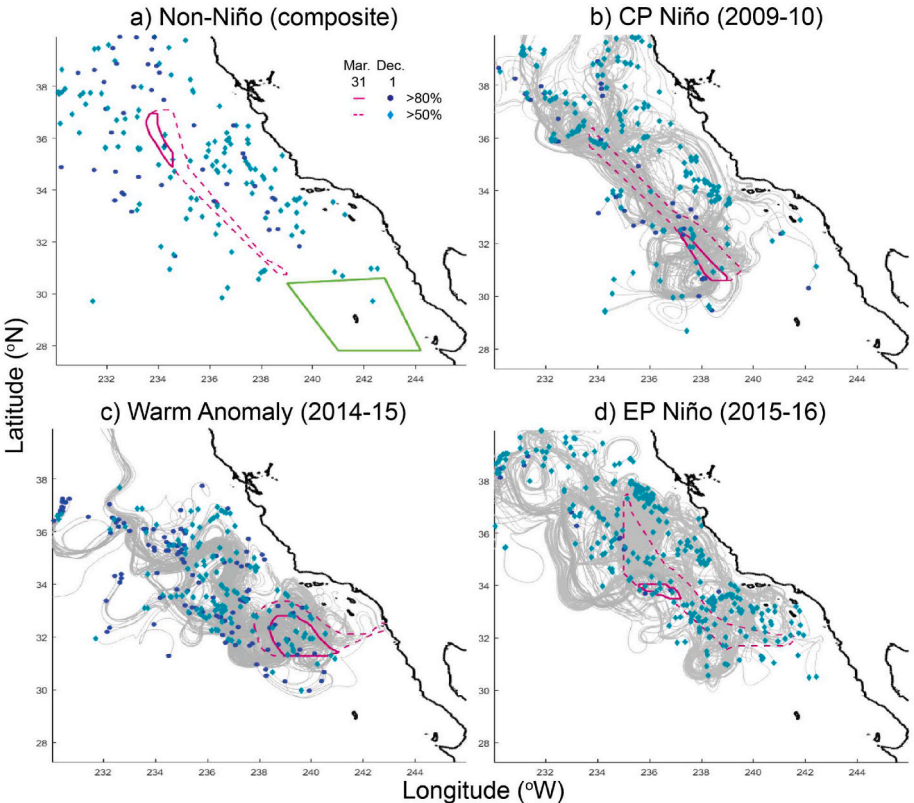


Fig. 11. As in Fig. 9, but for Euphausia gibboides. Euphausia gibboides was not detected in spring 2014, so panel 'a' only includes six years.

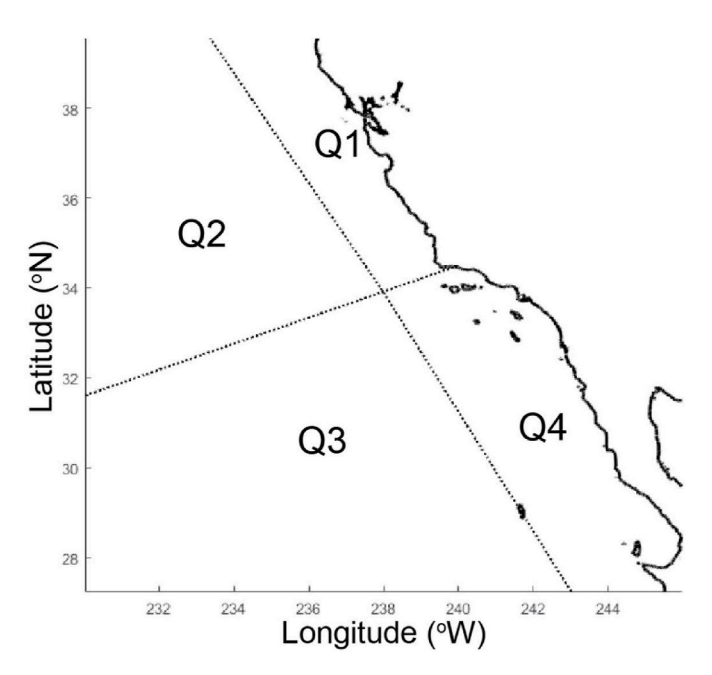


Fig. 12. The four CASE quadrants used to calculate particle proportions for December 1 backtracks (Fig. 13). Regions are as follows (see Section 2.4.3 for definitions): Q1 – Northern Inshore region; Q2 – Northern Offshore region; Q3 – Southern Offshore region; Q4 – Southern California Bight region. Q5 – particles backtracking outside of the CASE region (not shown on map).

reproduction, during anomalous years.

4.4. Limitations of current model setup

This study treated euphausiids as passive particles without biological behaviors such as vertical migration, swimming, or reproduction and mortality. We made this choice because measurements of *in situ* biological changes for most of these species do not currently exist. Essential next steps to refine the current findings are to include a vertical model dimension and to incorporate biological parameters as they become available for these species.

Additionally, our flow-biomass correlations evaluate relatively simplistic relationships between straight-line flows from potential sources and resulting changes in biomass; in reality, the CCS includes meanders and eddies that transport euphausiids on more circuitous paths, as demonstrated by our particle backtracks. However, our goal for this study was to examine large-scale, interannual relationships between regionwide flows and species biomass. We chose to use biomass anomalies, filtered flow fields, and pre-defined advection source flow boxes and directions in order to focus specifically on fluctuations in the biomass-flow relationships within our timeseries. Because our timeseries is limited in length and spatial observations, we sought to also limit the number of predictor variables we considered, to analyze only the relative variability in influence of advection on biomass. Our findings of correlations between species and flow even using large-scale averages and considering only relative anomalies indicates that flow-biomass relationships exist and our current methods capture at least some component of them. We present this study as a framework for future exploration of the relative influences of advection and other factors in determining euphausiid population fluctuations.

Finally, we note that we only examined one version (CASE) of modeled flow fields for the CCS. We chose this model because it has been

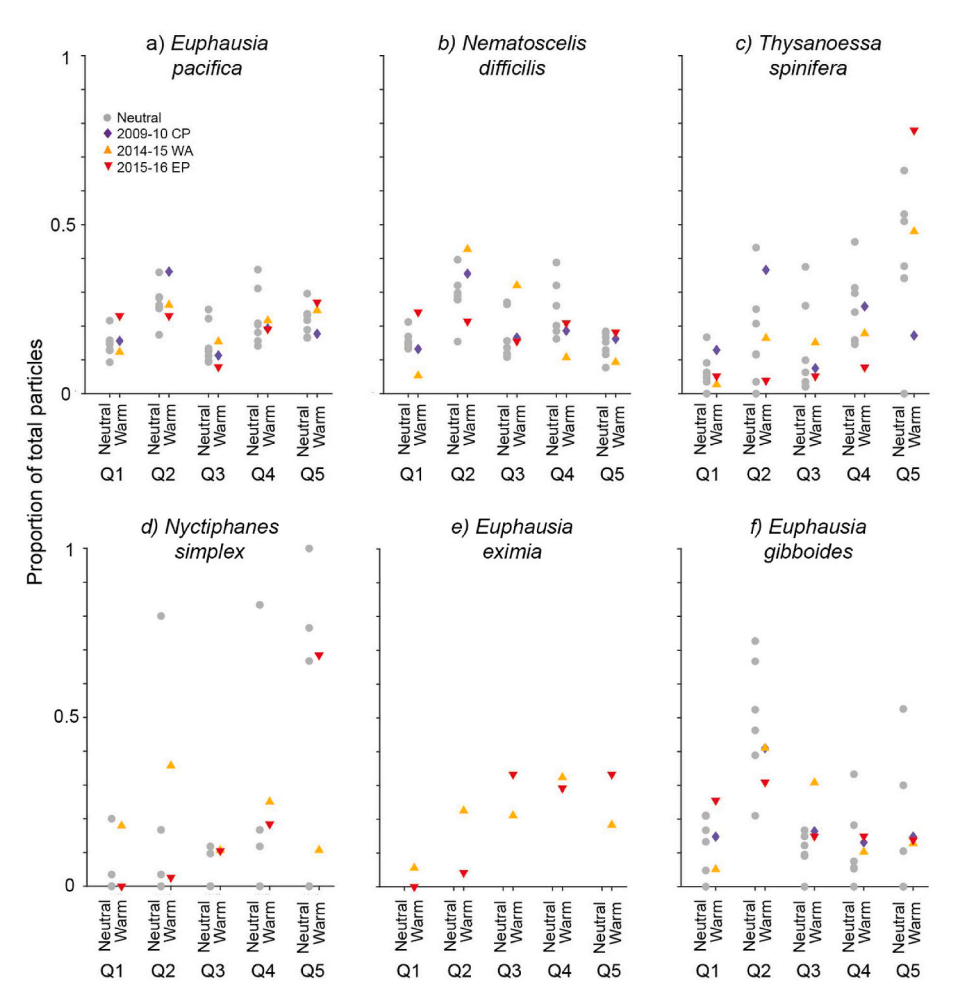


Fig. 13. Proportions of winter backtracked particles (blue and turquoise symbols in Figs. 6–11) that originated in each source quadrant for each species (see Fig. 12 for quadrant delineations; Q5 indicates particles that backtracked to outside the CASE model region). Proportions are calculated from the total number of particles seeded (sum of the >50% and >80% regions). The three anomalous years (colored symbols) are offset from all non-Niño years (light grey dots). Lack of symbols for *Nyctiphanes simplex* and *Euphausia eximia* indicate years of no presence.

optimized at mesoscale eddy resolution for the southern CCS region, via incorporation of actual *in situ* measurements and validation against CalCOFI physical data (see Section 2.2). A next step would be to conduct the same analyses using other modeled realizations of the CCS flow fields (e.g., HYCOM, ROMS) to produce a suite of correlation estimates and backtracks that could provide a fuller picture of the uncertainties associated with any particular circulation model.

4.5. Conclusions

This study sets out a quantitative framework for evaluating the effects of advection on euphausiid abundance. Our findings partially corroborate past hypotheses that resident cool-water species off central and southern California respond to El Niño-like perturbations primarily via *in situ* changes in population survival and reproduction, while nonresident subtropical-tropical species require initial transport into the region (Brinton, 1960; Brinton and Townsend, 1981; Marinovic et al., 2002; Lilly and Ohman, 2021). However, advection alone only partially describes fluctuations in subtropical species; not all years of apparently favorable flow actually result in increased biomass. We thus suggest that additional mechanisms or thresholds of flow are required to actually produce subtropical species increases in the Southern California Bight.

Our examination of differential adult and calyptopis (larval) relationships with flow highlights that resident cool-water species, in particular, likely shut off or turn on reproduction rapidly in response to changing habitat, regardless of current adult population levels. Continuing to refine our understanding of the ways in which source water advection influences different species, and the overall balances of *in situ* reproduction and population advection, will improve our ability

to effectively incorporate euphausiid species into future models of changing ocean food webs and biogeochemical cycles.

Author contributions

L.E.L. and M.D.O. developed the study. L.E.L. conducted all analyses. B.D.C. provided model access and substantial methodological assistance. All authors analyzed results and edited the manuscript. The authors declare no competing interests.

Declaration of competing interest

The authors declare that they have no known competing financial interests or personal relationships that could have appeared to influence the work reported in this paper.

Data availability

Links to codes and some data are available within manuscript. Other data available upon request.

Acknowledgements

We are indebted to G. Gopalakrishnan for development and further refinement of the California State Estimate, and to R. Musgrave and J. Garwood for generously sharing previous versions of the particle tracking model. We thank the CalCOFI program for at-sea sample collection and the late E. Brinton, as well as A. Townsend, and L. Sala of the Scripps Institution of Oceanography Pelagic Invertebrate Collection

(PIC) for detailed enumerations of euphausiid species. This work was supported by an NSF Graduate Research Fellowship to L. E. Lilly, NSF OCE-1614359 and OCE-1637632 to the California Current Ecosystem-LTER site, Gordon and Betty Moore Foundation support to M. D. Ohman, and NOAA Office of Naval Research support to B. D. Cornuelle and the CASE model. Supplemental animation files and associated codes and datafiles are available to view and download at https://doi.org/10.6075/JOKK9BZP (Lilly et al., 2022).

References

- Ainley, D.G., Hyrenbach, K.D., 2010. Top-down and bottom-up factors affecting seabird population trends in the California current system (1985-2006). Prog. Oceanogr. 84 (3.4) 242–254
- Bond, N.A., Cronin, M.F., Freeland, H., Mantua, N., 2015. Causes and impacts of the 2014 warm anomaly in the NE Pacific. Geophys. Res. Lett. 42 (9), 3414–3420.
- Brinton, E., 1960. Changes in the distribution of euphausiid crustaceans in the region of the California Current. CALCOFI (Calif. Coop. Ocean. Fish. Investig.) Rep. 7, 137–146
- Brinton, E., 1962. The Distribution of Pacific Euphausiids. Bulletin of the Scripps Institution of Oceanography, University of California, San Diego, pp. 51–270, 8.
- Brinton, E., 1981. Euphausiid distributions in the California Current during the warm winter- spring of 1977–78. In: The Context of a 1949–1966 Time Series, vol. 22.
 California Cooperative Oceanic Fisheries Investigations Reports, pp. 135–154.
- Brinton, E., Townsend, A., 2003. Decadal variability in abundances of the dominant euphausiid species in southern sectors of the California Current. Deep Sea Res. Part II Top. Stud. Oceanogr. 50 (14–16), 2449-2472.
- Brinton, E., Townsend, A.W., 1981. A comparison of euphausiid abundances from bongo and 1- m CalCOFI nets. Calif. Coop. Ocean. Fish. Investig. Rep. 22, 111–125.
- Brodeur, R.D., Hunsicker, M.E., Hann, A., Miller, T.W., 2019. Effects of warming ocean conditions on feeding ecology of small pelagic fishes in a coastal upwelling ecosystem: a shift to gelatinous food sources. Mar. Ecol. Prog. Ser. 617, 149–163.
- Butcher, J.C., 1987. The Numerical Analysis of Ordinary Differential Equations: Runge-Kutta and General Linear Methods. Wiley-Interscience.
- Capotondi, A., Wittenberg, A.T., Newman, M., Di Lorenzo, E., Yu, J.Y., Braconnot, P., Cole, J., Dewitte, B., Giese, B., Guilyardi, E., Jin, F.F., 2015. Understanding ENSO diversity. Bull. Am. Meteorol. Soc. 96 (6), 921–938.
- Chao, Y., Farrara, J.D., Bjorkstedt, E., Chai, F., Chavez, F., Rudnick, D.L., Enright, W., Fisher, J.L., Peterson, W.T., Welch, G.F., Davis, C.O., Dugdale, R.C., Wilkerson, F.P., Zhang, H.C., Zhang, Y.L., Ateljevich, E., 2017. The origins of the anomalous warming in the California coastal ocean and San Francisco Bay during 2014-2016. Journal of Geophysical Research-Oceans 122 (9), 7537–7557.
- Cheung, W.W.L., Frolicher, T.L., 2020. Marine. Heatwaves exacerbate climate change impacts for fisheries in the northeast Pacific. Sci. Rep. 10 (1).
- Cimino, M.A., Santora, J.A., Schroeder, I., Sydeman, W., Jacox, M.G., Hazen, E.L., Bograd, S.J., 2020. Essential krill species habitat resolved by seasonal upwelling and ocean circulation models within the large marine ecosystem of the California Current System. Ecography 43 (10), 1536–1549.
- Croll, D.A., Marinovic, B., Benson, S., Chavez, F.P., Black, N., Ternullo, R., Tershy, B.R., 2005. From wind to whales: trophic links in a coastal upwelling system. Mar. Ecol. Prog. Ser. 289, 117–130.
- Daly, E.A., Auth, T.D., Brodeur, R.D., Peterson, W.T., 2013. Winter ichthyoplankton biomass as a predictor of early summer prey fields and survival of juvenile salmon in the northern California Current. Mar. Ecol. Prog. Ser. 484, 203–217.
- Di Lorenzo, E., Ohman, M.D., 2013. A double-integration hypothesis to explain ocean ecosystem response to climate forcing. Proc. Natl. Acad. Sci. USA 110 (7), 2496–2499.
- Dorman, J.G., Powell, T.M., Sydeman, W.J., Bograd, S.J., 2011. Advection and starvation cause krill (Euphausia pacifica) decreases in 2005 Northern California coastal populations: implications from a model study. Geophys. Res. Lett. 38.
- Edwards, M., Beaugrand, G., Hays, G.C., Koslow, J.A., Richardson, A.J., 2010. Multidecadal oceanic ecological datasets and their application in marine policy and management. Trends Ecol. Evol. 25 (10), 602–610.
- Feinberg, L.R., Peterson, W.T., 2003. Variability in duration and intensity of euphausiid spawning off central Oregon, 1996-2001. Prog. Oceanogr. 57 (3–4), 363–379.
- Fisher, J.L., Menkel, J., Copeman, L., Shaw, C.T., Feinberg, L.R., Peterson, W.T., 2020. Comparison of condition metrics and lipid content between Euphausia pacifica and Thysanoessa spinifera in the northern California Current, USA. Prog. Oceanogr. 188.
- Frolicher, T.L., Fischer, E.M., Gruber, N., 2018. Marine. Heatwaves under global warming. Nature 560 (7718), 360—+.
 Gentemann, C.L., Fewings, M.R., Garcia-Reyes, M., 2017. Satellite sea surface
- Gentemann, C.L., Fewings, M.R., Garcia-Reyes, M., 2017. Satellite sea surface temperatures along the West Coast of the United States during the 2014-2016 northeast Pacific marine heat wave. Geophys. Res. Lett. 44 (1), 312–319.
- Gomez, J.G., 1995. Distribution patterns, abundance and population-dynamics of the euphausiids nyctiphanes-simplex and euphausia-eximia off the west-coast of Baja-California, Mexico. Mar. Ecol. Prog. Ser. 119 (1–3), 63–76.
- Jacox, M.G., Hazen, E.L., Zaba, K.D., Rudnick, D.L., Edwards, C.A., Moore, A.M., Bograd, S.J., 2016. Impacts of the 2015-2016 El nino on the California current system: early assessment and comparison to past events. Geophys. Res. Lett. 43 (13), 7072-7080.
- Kao, H.Y., Yu, J.Y., 2009. Contrasting eastern-pacific and central-pacific types of ENSO. J. Clim. 22 (3), 615–632.

- Keister, J.E., Johnson, T.B., Morgan, C.A., Peterson, W.T., 2005. Biological indicators of the timing and direction of warm-water advection during the 1997/1998 El Nino off the central Oregon coast, USA. Mar. Ecol. Prog. Ser. 295, 43–48.
- Lavaniegos, B.E., 1992. Growth and larval development of Nyctiphanes simplex in laboratory conditions. CALCOFI (Calif. Coop. Ocean. Fish. Investig.) Rep. 33, 162–171.
- Lavaniegos, B.E., Jiménez-Herrera, M., Ambriz-Arreola, I., 2019. Unusually low euphausiid biomass during the warm years of 2014–2016 in the transition zone of the California Current. Deep Sea Res. Part II Top. Stud. Oceanogr. 104638.
- Lavaniegos, B.E., Ohman, M.D., 2007. Coherence of long-term variations of zooplankton in two sectors of the California Current System. Prog. Oceanogr. 75 (1), 42–69.
- Lilly, L.E., Cornuelle, B.D., Ohman, M.D., 2022. Data from: Using a Lagrangian Particle Tracking Model to Evaluate Impacts of El Niño-Related Advection on Euphausiids in the Southern California Current System. UC San Diego Library Digital Collections.
- Lilly, L.E., Ohman, M.D., 2018. Cce IV: El niño-related zooplankton variability in the southern California current system. Deep-Sea Res. Part I Oceanogr. Res. Pap.
- Lilly, L.E., Ohman, M.D., 2021. Euphausiid spatial displacements elucidate El Niño forcing mechanisms in the southern California Current System. Prog. Oceanogr. 102544.
- Lilly, L.E., Send, U., Lankhorst, M., Martz, T.R., Feely, R.A., Sutton, A.J., Ohman, M.D., 2019. Biogeochemical anomalies at two southern California current system moorings during the 2014-16 warm anomaly-el Niño sequence. J. Geophys. Res.: Oceans.
- Lindegren, M., Checkley, D.M., Koslow, J.A., Goericke, R., Ohman, M.D., 2018. Climate-mediated changes in marine ecosystem regulation during El Nino. Global Change Biol. 24 (2), 796–809.
- Lynn, R.J., Bograd, S.J., 2002. Dynamic evolution of the 1997-1999 El nino-La nina cycle in the southern California current system. Prog. Oceanogr. 54 (1–4), 59–75.
- Marinovic, B.B., Croll, D.A., Gong, N., Benson, S.R., Chavez, F.P., 2002. Effects of the 1997- 1999 El Nino and La Nina events on zooplankton abundance and euphausiid community composition within the Monterey Bay coastal upwelling system. Prog. Oceanogr. 54 (1-4), 265–277.
- Marshall, J., Adcroft, A., Hill, C., Perelman, L., Heisey, C., 1997. A finite-volume, incompressible Navier Stokes model for studies of the ocean on parallel computers. J. Geophys. Res.: Oceans 102 (C3), 5753–5766.
- Matthews, S.A., Goetze, E., Ohman, M.D., 2020. Cross-shore Changes in Vertical Habitats of Mesozoplankton: A Paired Metabarcoding and Morphological Approach. Ocean Sciences Meeting 2020. AGU, San Diego, CA, USA.
- McClatchie, S., 2016. Regional Fisheries Oceanography of the California Current System. Springer.
- Miller, T.W., Brodeur, R.D., Rau, G., Omori, K., 2010. Prey dominance shapes trophic structure of the northern California Current pelagic food web: evidence from stable isotopes and diet analysis. Mar. Ecol. Prog. Ser. 420, 15–26.
- Nickels, C.F., Sala, L.M., Ohman, M.D., 2018. The morphology of euphausiid mandibles used to assess selective predation by blue whales in the southern sector of the California Current System. J. Crustac Biol. 38 (5), 563–573.
- Nickels, C.F., Sala, L.M., Ohman, M.D., 2019. The euphausiid prey field for blue whales around a steep bathymetric feature in the southern California current system. Limnol. Oceanogr. 64 (1), 390–405.
- Noaa, O.E.a.R., 2021. What Is an Expendable Bathythermograph, or "XBT"?.
- Pares-Escobar, F., Lavaniegos, B.E., Ambriz-Arreola, I., 2018. Interannual summer variability in oceanic euphausiid communities off the Baja California western coast during 1998-2008. Prog. Oceanogr. 160, 53–67.
- Ramp, S.R., McClean, J.L., Collins, C.A., Semtner, A.J., Hays, K.A.S., 1997. Observations and modeling of the 1991-1992 El Nino signal off central California. Journal of Geophysical Research-Oceans 102 (C3), 5553–5582.
- Roemmich, D., Johnson, G.C., Riser, S., Davis, R., Gilson, J., Owens, W.B., Garzoli, S.L., Schmid, C., Ignaszewski, M., 2009. The Argo Program: observing the global ocean with profiling floats. Oceanography 22 (2), 34–43.
- Ross, R.M., 1981. Laboratory culture and development of euphausia-pacifica. Limnol. Oceanogr. 26 (2), 235–246.
- Ross, R.M., 1982. Energetics of euphausia-pacifica .1. Effects of body carbon and nitrogen and temperature on measured and predicted production. Mar. Biol. 68 (1), 1–13.
- Ross, R.M., Daly, K.L., English, T.S., 1982. Reproductive-cycle and fecundity of Euphausia- pacifica in puget sound. Washington. Limnol. Ocean. 27 (2), 304–314.
- Rudnick, D.L., Zaba, K.D., Todd, R.E., Davis, R.E., 2017. A climatology of the California Current System from a network of underwater gliders. Prog. Oceanogr. 154, 64–106.
- Ruzicka, J.J., Brodeur, R.D., Emmett, R.L., Steele, J.H., Zamon, J.E., Morgan, C.A., Thomas, A.C., Wainwright, T.C., 2012. Interannual variability in the Northern California Current food web structure: changes in energy flow pathways and the role of forage fish, euphausiids, and jellyfish. Prog. Oceanogr. 102, 19–41.
- Santora, J.A., Mantua, N.J., Schroeder, I.D., Field, J.C., Hazen, E.L., Bograd, S.J., Sydeman, W.J., Wells, B.K., Calambokidis, J., Saez, L., Lawson, D., Forney, K.A., 2020. Habitat compression and ecosystem shifts as potential links between marine heatwave and record whale entanglements. Nat. Commun. 11 (1).
- Santora, J.A., Sydeman, W.J., Schroeder, I.D., Wells, B.K., Field, J.C., 2011. Mesoscale structure and oceanographic determinants of krill hotspots in the California Current: implications for trophic transfer and conservation. Prog. Oceanogr. 91 (4), 397–409.
- Schroeder, I.D., Santora, J.A., Moore, A.M., Edwards, C.A., Fiechter, J., Hazen, E.L., Bograd, S.J., Field, J.C., Wells, B.K., 2014. Application of a data-assimilative regional ocean modeling system for assessing California Current System ocean conditions, krill, and juvenile rockfish interannual variability. Geophys. Res. Lett. 41 (16), 5042, 5050.
- Stammer, D., Wunsch, C., Giering, R., Eckert, C., Heimbach, P., Marotzke, J., Adcroft, A. H., Marshall, J., 2002. Global ocean circulation during 1992–1997, estimated from

- ocean observations and a general circulation model. C.N. J. Geophys. Res.: Oceans
- Todd, R.E., Rudnick, D.L., Davis, R.E., Ohman, M.D., 2011. Underwater gliders reveal rapid arrival of El Nino effects off California's coast. Geophys. Res. Lett. 38. Von Storch, H., Zwiers, F.W., 2002. Statistical Analysis in Climate Research. Cambridge
- University Press.
- Zaba, K.D., Rudnick, D.L., 2016. The 2014-2015 warming anomaly in the Southern California Current System observed by underwater gliders. Geophys. Res. Lett. 43 (3), 1241–1248.
- Zaba, K.D., Rudnick, D.L., Cornuelle, B.D., Gopalakrishnan, G., Mazloff, M.R., 2018. Annual and interannual variability in the California current system: comparison of an ocean state estimate with a network of underwater gliders. J. Phys. Oceanogr. 48 (12), 2965–2988.